Proceedings of ICRC 2001: 1196 © Copernicus Gesellschaft 2001

ICRC 2001

A three-dimensional calculation of atmospheric neutrino fluxes

Y. Tserkovnyak[1], **R. J. Komar**[2], **C. W. Nally**[2], **and C. E. Waltham**[2]

[1]Physics Department, Harvard University, Cambridge MA 02138
[2]Department of Physics and Astronomy, University of British Columbia, Vancouver BC, Canada V6T 1Z1

Abstract. We present a fully three-dimensional calculation of atmospheric neutrino fluxes using accurate models of the geomagnetic field, hadronic interactions, tracking and decays. Results are presented for the Super-Kamiokande (SK) and Sudbury Neutrino Observatory (SNO) sites, and we make a comparison with previous one-dimensional calculations. The recently reported geometrical enhancement of low energy, horizontal neutrinos is confirmed, and east-west asymmetries calculated.

1 Introduction

Before the availability of cheap fast computers, calculations of atmospheric neutrino fluxes were either semi-analytical (Volkova 1980) or one-dimensional Monte Carlo simulations. There are two current major independent 1D calculations of atmospheric neutrino fluxes, that of the Bartol group ("BGS") (Barr 1989) and that of the "HKHM" group (Honda 1990). The main justification for the 1D approximation is that the transverse momentum from pion or muon decay is reckoned to be small enough (10's of MeV/c) to obviate the need to consider more dimensions when the threshold of the atmospheric neutrino detectors is at least 100 MeV/c.

Battistoni et al., (Battistoni et al. 2000) published the first results from a 3D calculation. They reported a geometrical enhancement of low energy, horizontal neutrinos. The origins of this effect were subsequently explained in a pedagogical paper by Lipari (Lipari 2000). The impact on the observed leptons is however, restricted to a small overall increase in flux and a small but significant improvement in understanding the so-called "east-west effect" seen in the Super-Kamiokande (SK) data (Lipari 2000). Other than this, neither our work nor Battistoni's report a large difference between the 1D and 3D approaches.

Correspondence to: C. E. Waltham
(waltham@physics.ubc.ca)

The newest large facility capable of observing atmospheric neutrinos is the Sudbury Neutrino Observatory (SNO). This water Čerenkov detector has about 2 kilotons in its active volume (about half D_2O and half H_2O). At 46.5° N (57.2° N magnetic) it is the most northerly atmospheric neutrino detector and hence the flux of low energy neutrinos will be larger than at more southerly sites like Super-Kamiokande (SK) at 25.8° N magnetic (Futagami 1999).

2 Theory

2.1 Introduction

In the absence of magnetic fields, the production of neutrinos by cosmic ray interactions in the earth's atmosphere can be calculated to a fair approximation by semi-analytic models (Volkova 1980). This is especially true at high energies, where the primary proton (or heavier nucleus), intermediate meson, and decay product muons and neutrinos, are all essentially co-linear. The mesons - mostly pions and kaons - have a choice of interaction or decay in the atmosphere, and the muons - if of low enough energy - can also decay. The cosmic ray primaries are isotropic; the only deviation from isotropy in the neutrinos is a horizontal enhancement due to a large slant range in the atmosphere, allowing more to decay.

$$P^{\pi,K,\mu}_{\nu_\mu+\bar{\nu}_\mu} = 285 \cdot \left(\frac{E}{\mathrm{GeV}}\right)^{-2.69} \cdot \left(\frac{1}{1+\frac{6E\cos\theta}{121\mathrm{GeV}}} + \frac{0.213}{1+\frac{1.44E\cos\theta}{897\mathrm{GeV}}}\right) /(\mathrm{m}^2\mathrm{sr.s.GeV}) \quad (1)$$

This expression, due to Volkova, gives the muon neutrino and antineutrino flux which results from π, K and μ decay. It is good to a few % at energies above 100GeV and angles not close to horizontal ($|\cos\theta| > 0.2$) where the curvature of the earth becomes important. We do not use this formula in our calculation, but it encapsulates the basic features of the neutrino flux.

2.2 Accounting for the Geomagnetic Field

Far away from the earth, where the geomagnetic field merges into the interplanetary field, the flux of cosmic rays is essentially isotropic (Barr 1988). As a cosmic ray approaches the earth, it is progressively bent by the geomagnetic field and, if it is of low enough rigidity (momentum/charge), it will be turned away. A typical value is that required for a particle to orbit the earth, just above the surface, at its magnetic equator, with a locally horizontal field of mean strength 25μT; this rigidity is 48GV/c (i.e. an energy of 48GeV for a proton). In addition, some parts of the earth's surface are, for certain angles and rigidities, in shadow from other parts of the earth.

We model these effects in a manner similar to that of the HKHM group (Honda 1990). The primary flux at large distances from the earth only depends on energy (and time - due to a small solar modulation, which we ignore for now) and can be written as $\phi_p^\infty(E)$. The primary flux which strikes the earth's atmosphere, however, depends on position and angle: $\phi_p(E, \mathbf{x}, \Omega)$. Invoking Liouville's theorem, which is applicable as long as the magnetic field can be considered static, yields the simple form:

$$\phi_p(E, \mathbf{x}, \Omega) = \phi_p^\infty(E) \text{ for allowed paths} \quad (2)$$
$$= 0 \text{ for forbidden paths} \quad (3)$$

To decide which paths are allowed or forbidden, a check is made for shadowing by the earth before a positively charged primary is tracked through the atmosphere. An equivalent negatively charged particle is tracked backwards to see if its trajectory reaches a very large distance from the earth without intersecting with it. If it did, such a trajectory is allowed, if not, it is rejected.

For any given position on the earth's surface, an angular map may be made showing the minimum rigidity required for a positively charged particle, starting from a large distance away, to reach the surface from that angle. Such maps for the SK and SNO sites are shown in Fig. 1. The more northerly SNO site has in general much lower cutoffs. The SNO site has the opposite up-down asymmetry to the SK site, and a very much smaller east-west asymmetry. In terms of cardinal points the x-axis is ordered N-W-S-E-N.

2.3 Input Parameters: Primary Flux, Geomagnetic Field and Earth's Atmosphere

Atmospheric neutrino calculations are dependent on various physical models. Most of the uncertainty, which is estimated as 20%, is introduced by our knowledge of the primary cosmic ray spectrum. For this we use the same parameterization (Webber/Lezniak) as for the Bartol calculation (Agrawal et al. 1996, Gaisser et al. 1996), and assume medium solar activity. The geomagnetic field is calculated using a 10th order multipole expansion, with spherical harmonic coefficients taken from the IGRF (IGRF 1995) model. Errors in the field at the earth's surface are less than 25 nT (<0.1%). The atmospheric density is calculated according to Linsley's compilation of atmospheric density data (Linsley 1976).

2.4 Tracking Primaries and Secondaries

Inside the atmosphere both primaries and secondaries were tracked in steps of 1 km. In each case helical steps were taken, using the magnetic field at the centre of the helix and assuming it to be uniform over the step. In order to keep statistics sensible, detector areas were artificially increased to a rectangle 5° by 10° with the shorter side pointing to magnetic north to reduce the washing out of local geomagnetic effects. The "detector" was considered to be a flat sheet as any increase in the thickness was found to wash out the geometrical horizontal enhancement.

2.5 Hadronic Interactions

Simulation of the interactions between primaries and air nuclei, and the subsequent interactions and decays of secondaries, was carried out largely with the GEANT-FLUKA package (Fassò 1993).

2.6 East-West Effect

As Lipari has pointed out (Lipari 2000), there is a hierarchy in the asymmetries of the different neutrino species, due to the difference in the bending of primaries and secondaries. The ν_e arises from the decay of positively charged secondaries and so the asymmetry is the largest. The $\bar{\nu}_e$ arises from the decay of negatively charged secondaries and so the asymmetry is the smallest. In between lie the $\bar{\nu}_\mu$ and ν_μ, with the former having a larger asymmetry as some of them arise from decaying positive muons which are more deflected than neutrinos produced directly from pion decays.

The effect is not easy to find in the data without energy and directional cuts. Lipari proposes using neutrinos which produce leptons with energies of 0.4-3GeV with zenith angles $|\cos\theta_l < 0.5|$. The standard definition of the asymmetry A in terms of the numbers of neutrinos $N_{E,W}$ is as follows.

$$A = \frac{N_E - N_W}{N_E + N_W} \quad (4)$$

With a 3D calculation he obtains an electron E-W asymmetry for the SK site of 0.224 and a muon asymmetry of 0.091. The corresponding experimental values are in good agreement, being 0.21 ± 0.04 and 0.08 ± 0.04 respectively.

3 Results

3.1 East-West Effect

Our model reproduces the correct hierarchy of East-West asymmetries, in order of highest to lowest: $\nu_e, \bar{\nu}_\mu, \nu_\mu, \bar{\nu}_e$. However, our values are significantly higher than those of Lipari (Lipari 2000), and produce an overall electron asymmetry of

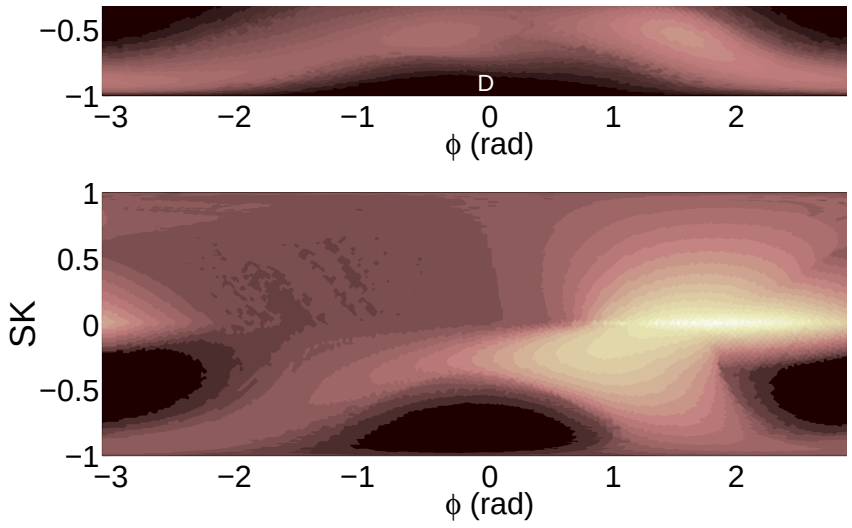

Fig. 1. Rigidity cutoffs in the 1D model for SNO (top) and SK (bottom) sites. The more northerly SNO site has in general much lower cutoffs. The SNO site has the opposite up-down asymmetry to the SK site, and a very much smaller east-west asymmetry. These cutoffs were not used in the calculation, they are merely means to check part of the code, and as an aid to understanding. In terms of cardinal points the x-axis is ordered N-W-S-E-N.

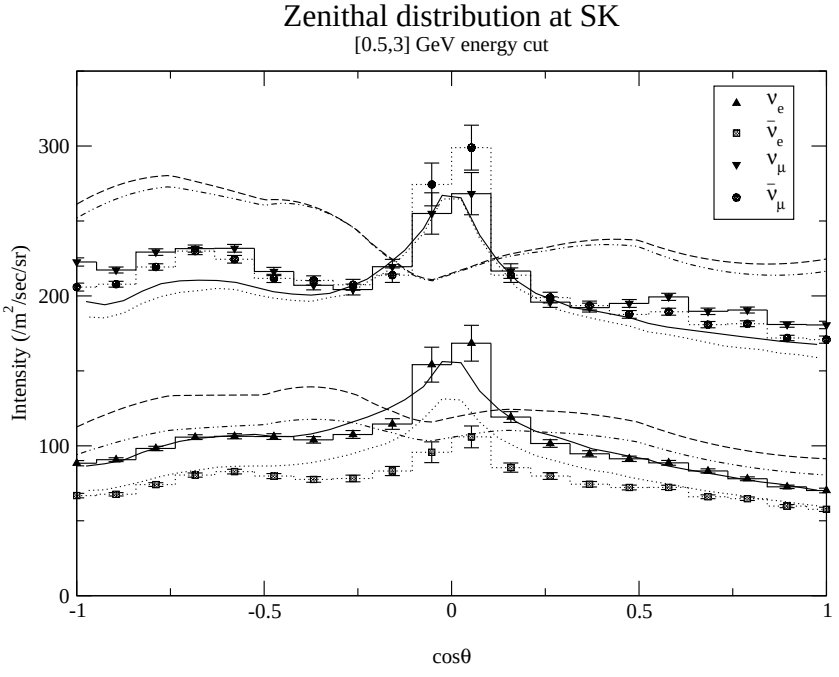

Fig. 2. Zenith angle distributions for SK site. The data points are this work, as shown in the figure. The lines are other calculations. Those with the horizontal peak are from the 3D model of Battistoni et al. (Battistoni 2000); the solid lines are neutrinos and the dotted antineutrinos. The lines with the slight horizontal dip are from the Bartol 1D model (Agrawal 1996); the dashed lines are neutrinos and the dash-dotted antineutrinos.

0.3, and a muon asymmetry of 0.2. The cause of this disagreement is still being investigated.

3.2 Horizontal Enhancement

Figures 2 and 3 show the zenith angle distributions (0.5 GeV$<$ E_ν $<$3 GeV) for the SK and SNO sites for our calculations, and those of Bartol (1D) and Battistoni (3D). Lipari's horizontal enhancement can be seen in the 3D models, especially at the SNO site where neutrino spectrum is much softer. This feature is not present in the 1D calculation, however, it is almost completely washed out in the detection of neutrino-induced leptons.

4 Conclusion

One-dimensional calculations of atmospheric neutrino fluxes have served us very well and reproduce most data, once neutrino oscillations are taken into account. The approximation does not seem to introduce a serious systematic error into the conclusion that neutrino oscillations are taking place. However, the large amount of data currently being amassed by SK and other detectors mean that second order effects can now be investigated, and these are beginning to require 3D

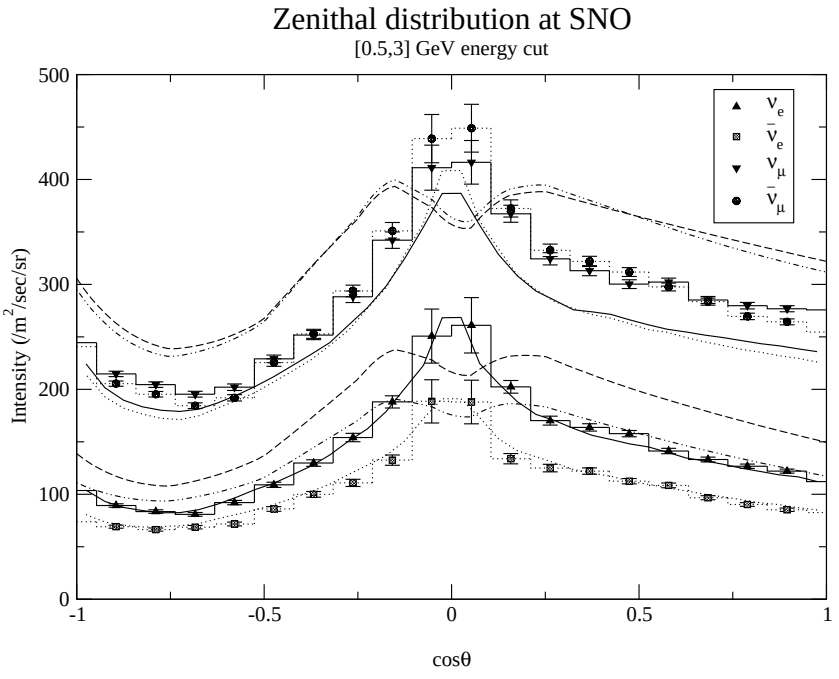

Fig. 3. Zenith angle distribution for SNO site. Line convention as for SK. The horizontal enhancement is greater at SNO than at SK because the higher geomagnetic latitude softens the neutrino spectrum.

calculations.

Acknowledgements. The authors would like to thank Ed Kearns and Chris Walter for the use of the Boston University Physics Department's O2000 CPU farm. We also thank Thomas Gaisser and Paolo Lipari for useful discussions. The work was supported by the Natural Science and Engineering Research Council of Canada (NSERC). One of us (YT) is grateful for a Faculty of Science scholarship from the University of British Columbia, and a summer studentship from the TRIUMF laboratory.

References

V. Agrawal, T. K. Gaisser, P. Lipari and T. Stanev, Phys. Rev. D **53**, (1996) 1314.

G. Barr, T. K. Gaisser and T. Stanev, Phys. Rev. **D38**, 85-94 (1988).

G. Barr, T. K. Gaisser and T. Stanev, Phys. Rev. **D39**, 3532 (1989).

G. Battistoni, A. Ferrari, P. Lipari, T. Montaruli, P. R. Sala and T. Rancati, Astroparticle Physics **12** (2000) 315-333.

A. Fassò, A. Ferrari, J. Ranft and P. R. Sala, Proc. IV Int. Conf. on Calorimetry in High Energy Physics, La Biodola (Elba), Ed. A. Menzione and A. Scribiano, World Scientific p.493 (1993).

T. Futagami *et al.* (Super-Kamiokande collaboration), Phys. Rev. Lett. **81**, 1562 (1998).

T. K. Gaisser, "Cosmic Rays and Particle Physics", (Cambridge 1992), p.85ff.

T. K. Gaisser, M. Honda, K. Kasahara, H. Lee, S. Midorikawa, V. Naumov and T. Stanev, Phys. Rev. **D54**, 5578 (1996).

M. Honda, K. Kasahara, K. Hidaka and S. Midorikawa, Phys. Lett. **B248**, 193 (1990).

IGRF website: http://www.ngdc.noaa.gov/seg/potfld/geomag.html

Linsley standard atmosphere 1976, NASA technical report NASA-TM-X-74335, NOAA technical report NOAA-S/T-76-1562 (1976)

P. Lipari, Astropart. Phys. **14** (2000) 153-170 and 171-188.

L. V. Volkova, Sov. J. Nucl. Phys. **31** (1980) 784-790.